SUPPLEMENT TO THE *WELDING JOURNAL*, AUGUST 2012
Sponsored by the American Welding Society and the Welding Research Council

Effect of the Consumable on the Properties of Gas Metal Arc Welded EN 1.4003-Type Stainless Steel

The properties of a modified 12% Cr ferritic stainless steel were evaluated when welded with three different consumables

BY E. TABAN, A. DHOOGE, E. KALUC, AND E. DELEU

ABSTRACT

In this study, modified 12% Cr stainless steel with very low carbon level (0.01%) to improve the weldability and mechanical properties, still conforming to EN 1.4003 and UNS S41003 grades, was joined by gas metal arc welding. Plates 12 mm thick were welded with ER309LSi, ER308LSi, and ER316LSi austenitic stainless steel consumables. Several samples extracted from the joints were subjected to mechanical testing by means of tensile, bend, and Charpy impact toughness tests, while tensile fractographs were examined. Toughness after the postweld heat treatment (PWHT) for 30 min at 720° and 750°C was also examined. Microstructural examinations, including macro- and micrographs, grain size analysis, hardness, and ferrite measurements, were conducted. Salt spray and blister tests for corrosion testing were applied. Considering all data obtained, good strength and satisfactory ductility results were determined, while microstructure-property relationship was explained. It can be recommended to use 309 and 316 welding wires for better corrosion resistance compared to 308 welding wires. More encouraging impact toughness properties related with finer grained microstructure were also obtained for the welds produced by 309 and 316 wires. Postweld heat treatment of the GMA weld with ER308LSi showed good improvement for toughness due to the tempering of the martensite at the coarse-grained heat-affected zone. Increasing heat treatment temperature from 720° to 750°C made additional improvements in toughness.

Introduction

Ferritic stainless steels are gaining more interest because they exhibit good corrosion resistance and lower cost compared to austenitic stainless steels. Low-chromium grades have fair corrosion resistance and low cost fabricability, and they have been widely used in automotive exhaust systems. The fact that a fully ferritic structure has poor low-temperature toughness and poor high-temperature strength compared to austenite led these steels to be considered as low-weldable steels, and they have mostly been used for applications that do not require welding. In recent years, there has been an increased use of fusion welding in such industrial applications, hence the welding metallurgy of ferritic stainless steels has drawn more attention. However, in joining ferritic stainless steels, a grain-coarsening problem occurs at the weld zones and, consequently, low toughness and ductility due to the absence of phase transformation. The performance potential of lean alloyed chromium stainless steels has been increased with the tight control of composition that can provide extremely low levels of carbon and nitrogen with the consequent improvement in the as-welded heat-affected zone (HAZ) properties, as well as the reduction of chromium carbides, which degrade corrosion performance (Refs. 1–17).

In some predominantly ferritic steels, a small amount of austenite forms at high temperatures and may transform to martensite on cooling. With this idea, 12% Cr transformable stainless steels, potentially with better weldability than either ferritic or martensitic steels, were developed with tight control of the carbon content and martensite/ferrite balance to avoid the extremes of completely ferritic or martensitic structures. These structured stainless steels with low carbon and interstitials have been finding increasing engineering applications (i.e., vs. S355 steel), depending on the improvements in weldability. The first generation of these ferritic steels is 3Cr12 stainless steel, which was developed in the late 1970s with a carbon level of 0.03%. It is produced by several steel suppliers and is named in ASTM A240 as UNS S41003 and in European Standards as Material Number 1.4003. This 3Cr12 is variously described as ferritic or ferritic-martensitic 12% Cr stainless steel with good corrosion resistance in many environments and provides considerable economic advantage over austenitic stainless steels (Refs. 1, 4, 11, 12, 18–28). Although 3Cr12 has excellent corrosion resistance in many environments, its limited weldability and relatively low impact toughness at the HAZ have restricted its use where nonstatic loads are concerned.

*E. TABAN (*emel.taban@yahoo.com, emelt@kocaeli.edu.tr*) and E. KALUC are with Dept. of Mechanical Engineering, Faculty of Engineering, Kocaeli University, Kocaeli, Turkey, and Welding Research Center, Kocaeli University. E. TABAN was a PhD student at the Research Center of the Belgian Welding Institute, Ghent, Belgium at the time this study was conducted. A. DHOOGE is with Dept. of Mechanical Construction and Production, Faculty of Engineering and Architecture, University of Ghent, Ghent, Belgium. E. DELEU is with Research Center of the Belgian Welding Institute, Ghent, Belgium.*

KEYWORDS

12% Cr Stainless Steel
EN 1.4003 Steel
Gas Metal Arc Welding
Microstructure
Impact Toughness
Corrosion Resistance

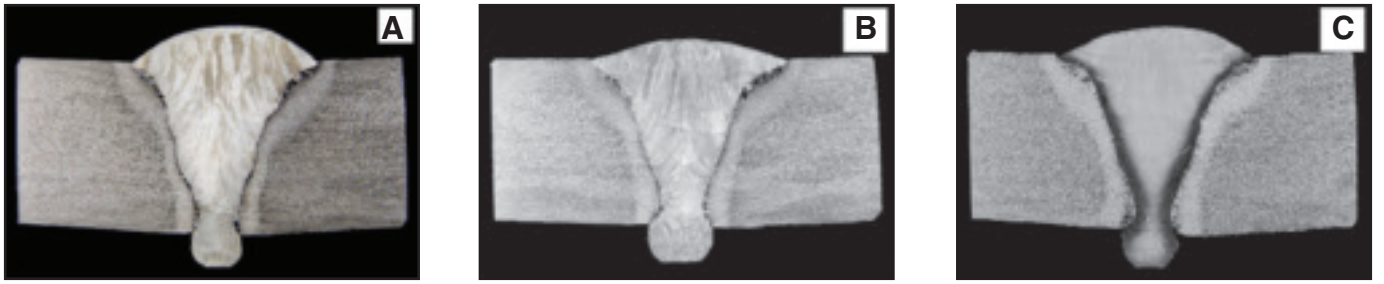

Fig. 1 — Photo macrographs of welded joints. A — B9; B — B8; C — B6.

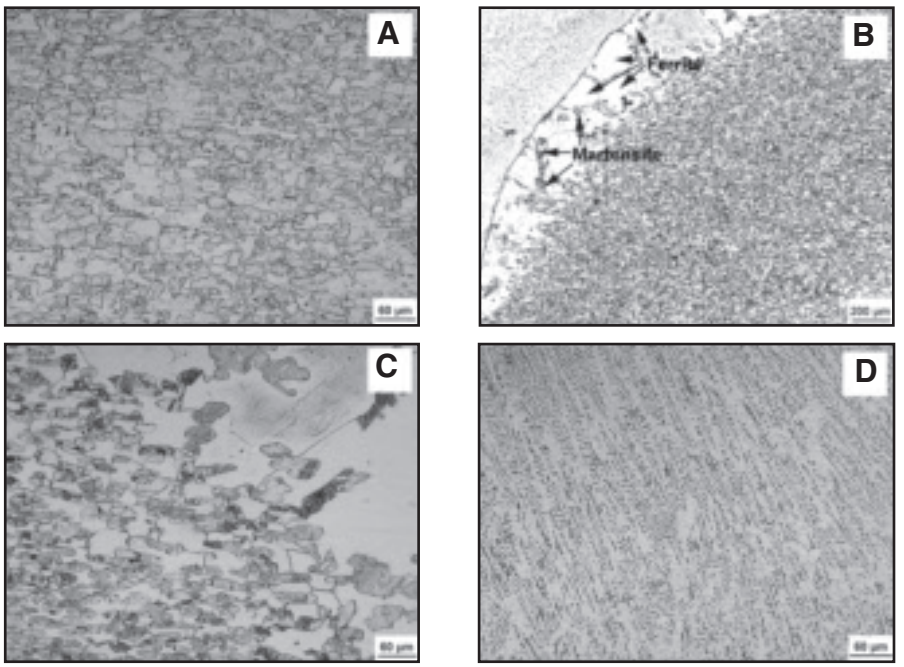

Fig. 2 — Photomicrographs of GMA weld with 309 filler metal (B9). A — BM, 200×; B — WM+HAZ, 50×; C — HAZ, 200×; D — WM, 200×.

The correct balance between ferrite- and austenite-forming elements is very important, and this can be controlled using certain relationships based on the ferrite- or austenite-forming tendencies of alloying elements, depending on both alloying and heat treatment conditions (Refs. 6, 19, 25–36). A modified 12%Cr stainless steel was fabricated conforming in composition to Grade EN 1.4003 with quite low (<0.015%) carbon levels, improving weldability and mechanical properties with modern production facilities. Initial applications of this steel were limited to materials handling equipment in corrosive environments, but the 1.4003 steel is now used commonly in the coal and gold mining industries, for sugar-processing equipment, road and rail transport, power generation, and in aerospace engineering.

Table 1 — Chemical Composition and Tensile Properties of the Base Metal

Chemical Composition (wt-%) (data from chemical analysis)[a]						
C	Si	Mn	P	S	Cr	Ni
0.01 [≤ 0.030]	0.32 [≤ 1.00]	0.97 [≤ 1.50]	0.033 [≤ 0.04]	0.003 [≤ 0.015]	12.2 [10.5–12.5]	0.52 [0.30–1.00]
N (ppm) 90 [≤ 300]	Cu 0.39	Mo 0.14	Ti 0.001	V 0.039	Al 0.027	Nb 0.031

Yield strength (MPa)	Ultimate tensile strength (MPa)	Strain at fracture (%)
362–363	500–502	30–32

(a) Values between square brackets are as specified in EN10088.

This 1.4003 steel is considered a link between carbon steels and corrosion-resistant alloys since it displays both the advantages of stainless steels for corrosion resistance and the engineering properties of carbon steels. For the long-term maintenance costs, this modified low-carbon 12Cr stainless steel requires less coating renewals, offering substantial economic and considerable environmental advantages. For other applications, when compared with higher-alloyed stainless steels, the use of this steel with improved weldability would be more economical (Refs. 12, 16–19, 23, 25, 35–49). Modified lower-carbon 12Cr stainless steel (0.01%) is intended to be used for structural applications, so welding and weldability of this alloy gains more importance.

This study aims to investigate the weldability properties of this steel. The properties of gas metal arc welded modified 12% Cr ferritic stainless steel joints with various types of consumables (ER309LSi, ER308LSi, and ER316LSi) were investigated. Microstructural, mechanical, impact toughness, and corrosion testing were carried out to determine the gas metal arc weldability of this steel, and the results were compared to evaluate the effect of consumable type on the properties of the welded joints.

Material and Experimental Procedure

Material

The chemical composition and transverse tensile properties of the 12-mm-thick modified base metal are given in Table 1. Chemical composition data were obtained by glow discharge optical emission spectrometry (GDOES), and nitrogen was determined by melt extraction.

Welding

Three types of gas metal arc welded joints (B9, B8, and B6) of modified EN 1.4003 steel with various types of consumables were produced. Matching welding electrodes and 17% Cr welding wires are available for welding of EN 1.4003 steel. However, in applications where impact, fatigue, or any other form of nonstatic load-

ing is anticipated, mainly austenitic welding wires are recommended. Reported weldability studies have shown that austenitic stainless steel consumables can be used to produce arc welds to minimize the risk of HAZ hydrogen cracking and to ensure deposition of tough weld metal to yield adequate properties required for structural purposes (Refs. 12, 15, 18, 19, 23, 35, 41–49). Weld B9 was prepared with a solid ER309LSi wire of 1-mm diameter protected by a slightly oxidizing EN 439-M12(2) gas and by using pulsed arc. The plate preparation consisted of a V-groove with an opening angle of 50 deg. Four passes were used to complete the weld, supported by a copper backing strip. No preheat was applied, while the maximum interpass temperature was 100°C. The heat input varied from 0.41 to 1.73 kJ/mm. The same conditions were applied for GMAW with ER308LSi and ER316LSi solid wires respectively for Welds B8 and B6. The heat input in these cases changed respectively from 0.68 to 1.90 kJ/mm and from 0.53 to 1.73 kJ/mm. The maximum interpass temperatures were 115° and 118°C. Welding details of the joints are given in Table 2.

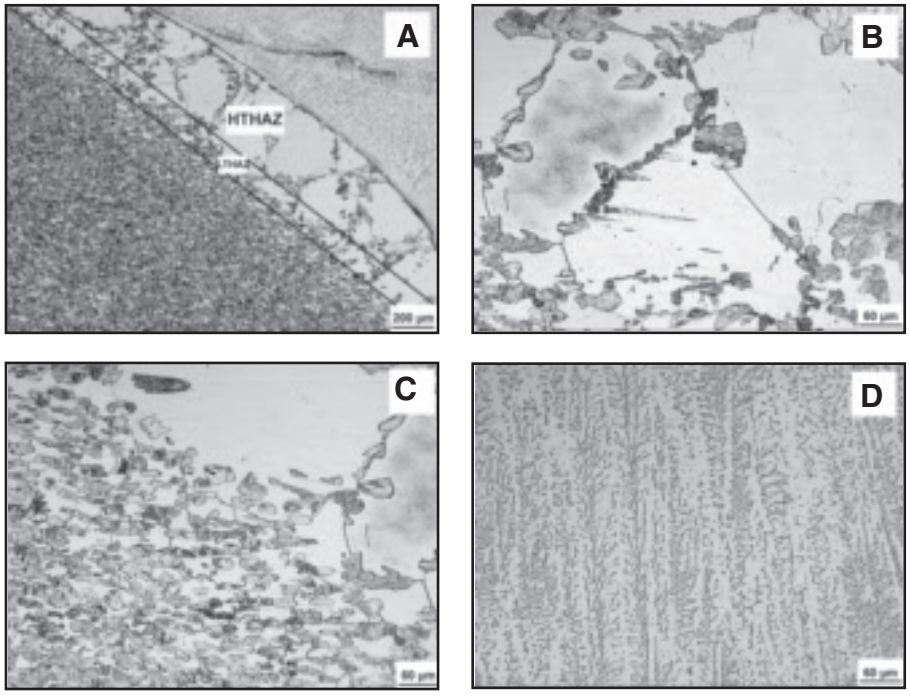

Fig. 3 — Photomicrographs of GMA weld with 308 filler metal (B8). A — WM+HAZ, 50×; B — HTHAZ, 200×; C — HAZ, 200×; D — WM, 200×.

Microstructural, Mechanical, and Corrosion Testing of the Welded Joints

For the chemical analyses of the weld deposits, longitudinal sections were prepared perpendicular to the plate surface and entirely located at the weld metal. At least two measurements were done by GDOES, and nitrogen was again determined by melt extraction. Welded joints were cross-sectioned perpendicular to the welding direction for metallographic analyses. Specimens were prepared, polished and etched with Vilella's reagent. Photomacro and photomicrographs of the weld zones were obtained by light optical microscope (LOM) with magnifications of 50 and 200×.

Notch impact test samples were extracted transverse to the weld with notches positioned at the weld metal (WM) center, at the weld interface (WI), at the HAZ 2 mm away from the WI (WI+2 mm). Testing was carried out at –20°, 0°, and 20°C. The impact test samples were also tested at –20°C after PWHT for 30 min respectively at 720° and 750°C. The ASTM

Table 2 — Welding Details Applied for Gas Metal Arc Joining the 12-mm-Thick Base Metals

Weld Joint	Welding Position	Type of Consumable	Protection	Plate Preparation	Backing Material	Welding Parameters (V/A)	Welding Speed (cm/min)	Heat Input (kJ/mm)	Preheat Temp. (°C)	Interpass Temp. (°C)
B9		(1mm diameter) ER309LSi				20.0–24.5/ 100–153 Pulsed arc	30/13	0.41/1.73	—	≤100
B8	PA 4 passes	(1mm diameter) ER308LSi	63Ar/ 35He/ 2CO_2	V / 50° (c= 2–4 mm)	Cu	23.0–29.0/ 100–178 Pulsed arc	25/16	0.68/1.90		≤115
B6		(1mm diameter) ER316LSi				22.0–27.5/ 90–185 Pulsed arc	30/18	0.53/1.73		≤118

Table 3 — Chemical Compositions of the Weld Deposits Made for the GMA Welds

Weld Joint	C (%)	Si (%)	Mn (%)	P (ppm)	S (ppm)	Cr (%)	Cu (%)	Ni (%)	Mo (%)	Ti (ppm)	V (ppm)	Al (ppm)	Nb (ppm)	N (ppm)
B9	0.02	0.79	1.80	180	70	23.6	0.04	12.9	0.04	80	1100	280	<10	524
B8	0.02	0.76	1.51	210	70	20.0	0.10	9.79	0.10	50	790	280	10	653
B6	0.03	0.72	1.56	230	120	18.6	0.15	11.9	2.52	40	820	260	<10	474

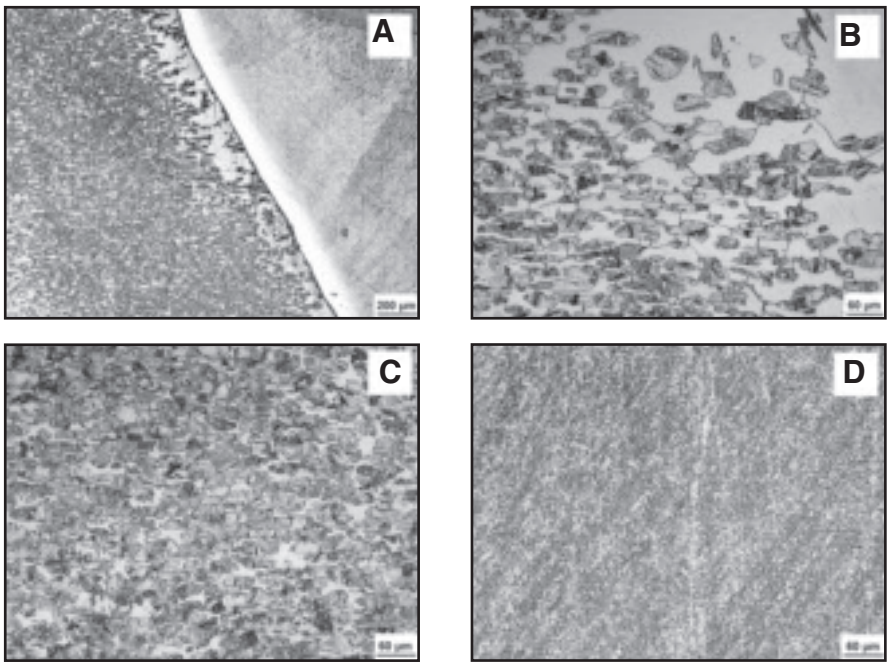

Fig. 4 — Photomicrographs of GMA weld with 316 filler metal (B6). A — WM+HAZ, 50×; B — HAZ, 200×; C — LTHAZ, 200×; D — WM, 200×.

grain size numbers were measured at positions sampled by notches located at WI and WI+2 to investigate for a possible correlation between toughness and microstructure.

Ferrite content of the weld metal was calculated and predicted by chemical analysis results, then was determined by Feritscope® measurements across the weld metal. Vickers hardness measurements under 5-kg load were carried out over the weld cross sections in accordance with the EN 1043-1 standard. Transverse, full-thickness, rectangular tensile test specimens were extracted from the welds and testing was performed with a 600-kN capacity servo-hydraulic test machine at room temperature. The width at the prismatic section was 25 mm, while the excess flush of the weld metal was removed in order not to overestimate the weld metal strength. Cylindrical test samples, completely positioned at the weld metal were prepared in the longitudinal direction. Moreover, transverse face and root bend test specimens with a nominal specimen width of 30 mm were prepared. Bending was executed to 180 deg unless severe cracking was observed before.

To assess the resistance against atmospheric attack, salt spray and blister corrosion tests were executed. Salt spray tests were done on the corrosion test samples, which were coated with a two-layer protection system used in the industry. Testing was applied in a 5% NaCl aqueous solution with a fog volume of 24 to 28 mL per 24 h, a pH of 6.5 to 7.2, and at a temperature of 35°C. The samples were provided with a scratch in the shape of a cross over the entire test surface across the weld metal surface to estimate the resistance of the welds when the coating is accidentally damaged prior to or during operation and also with paraffin at the sawed and machined surfaces. Samples with a dimension of 150 × 75 mm were positioned at 60 deg with the weld horizontal. Blister tests were executed on coated samples prepared similarly as those for salt spray testing. Samples were exposed to real atmospheric conditions at the center of Gent/Belgium with their test surface oriented to direct sunlight.

Table 4 — Full-Thickness Transverse Tensile Properties of the 12-mm-Thick GMA Welds

Welding Process	Type of Consumable	Specimen Code	R_m (MPa)
GMAW	ER309LSi	B9TT1	484
		B9TT2	504
	ER308LSi	B8TT1	491
		B8TT2	492
	ER316LSi	B6TT1	490
		B6TT2	499

Results and Discussion

Chemical Analysis

Chemical composition of the weld deposits of gas metal arc welded joints are given in Table 3. Data were obtained by the experimental analysis (GDOES and melt extraction) from the top passes of the weld metal.

More chromium and nickel were measured at the weld metal of Weld B9 compared to the welds produced with 308 and 316 filler metals. On the other hand, more Mo was determined at the B6 weld due to the increased alloying elements of the related wire.

Microstructural Analysis

A microstructural investigation was carried out on the metallographic specimens from the joints. Relevant macrophotographs obtained from each joint are given in Fig. 1. All welds show a reasonable weld profile.

An investigation of the weld zones was performed from base metal (BM) across the HAZ to weld metal (WM) (Figs. 2, 3, and 4, respectively, for B9, B8, and B6 joints).

The base metal used in this study is often described as a ferritic or ferritic/martensitic stainless steel since it includes both ferrite and martensite in the base metal structure — Fig. 1A. Unlike the HAZ for plain carbon steels, the HAZ for 12%Cr stainless steels has two visually distinct zones: the high-temperature HAZ (HTHAZ) and the low-temperature HAZ (LTHAZ) — Figs. 1B, 2A, 3A. The steel is heated close to the liquidus and transforms completely to δ ferrite and rapid grain growth occurs. On cooling, the HTHAZ frequently consists of coarse-grained δ ferrite with islands of martensite at the grain boundaries. On the micrographs, martensite islands can be observed, and adjacent to the weld interface some grain coarsening at the HAZ of the stainless steel was observed — Figs. 1C, 2B, 3B. When the material temperature reached 1050°C within 1–2 s, no reversion to γ occurred, and the δ ferrite structure was maintained at room temperature. However, material that was heated between Ac1 and Ac5, and contained significant fractions of γ, transformed to martensite, resulting in a tough fine-grained structure (Refs. 19, 28). The base metal had the tendency for grain coarsening at the HAZ close to the weld interface where temperature cycles occur with peak temperatures above 1200°C if the heat input during welding is not properly controlled. This is due to the transformation to ferrite in the HTHAZ of fusion welds.

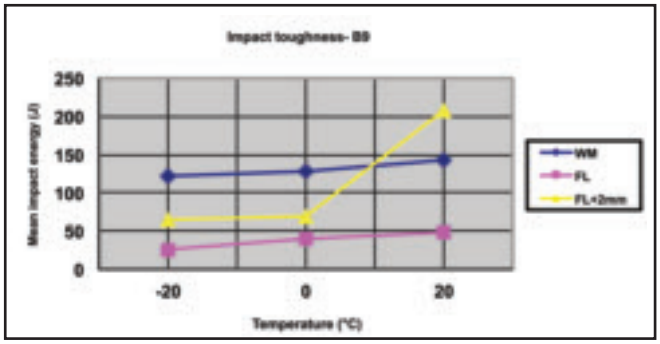

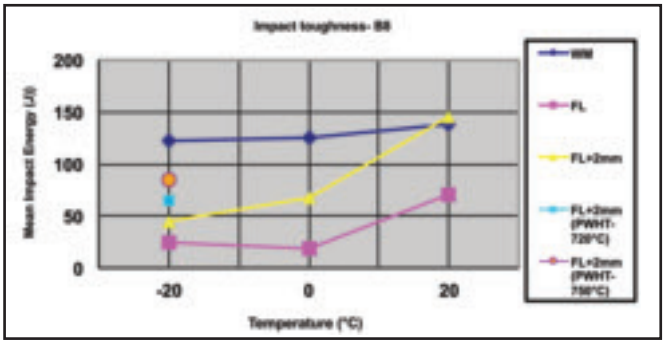

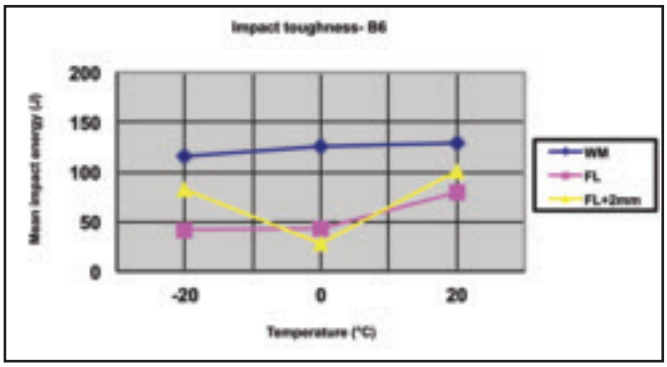

Fig. 5 — Notch impact toughness of the GMA welded joints (B9, B8, and B6).

Impact Toughness Test Results

Curves of Charpy impact energies vs. test temperature for the 12-mm-thick GMA welded joints (B9, B8, and B6) with 309, 308, and 316 consumables are given in Fig. 5. Considering 27 J as the required mean toughness, it could be concluded that all welds proved adequate for low-temperature impact toughness (achievable down to –20°C, which is very encouraging). Each point in the figure represents an average value of three samples. However, only the samples with weld interface (WI) notch position of B8 weld tested at low temperatures failed. The PWHT of the B8 weld for 30 min at 720° and 750°C showed good improvement for HAZ toughness. With increasing the heat treatment temperature from 720° to 750°C, results improved — Fig. 5. Similar Charpy impact toughness test results were obtained for WM notched samples, while samples removed from welds notched at the WI and WI+2 positions possessed less impact energy results compared to WM positions. In general, better impact toughness results were obtained at the weld produced with 316 welding wires for all test temperatures. As the alloying elements increase in 309 and 316 filler metals, the alloying of the weld metal improved, and more encouraging results were obtained in B9 and B6 welds.

Grain Size Analysis

Grain coarsening in the fusion welds of this steel results in deterioration of mechanical properties, in particular of toughness, as also observed in earlier research (Refs. 12, 41–50). Considering this, ASTM grain size numbers were measured on the existing macrosections at the HAZ close to the weld interface to investigate for a correlation between impact toughness and grain size of the welds. It is emphasized that fine-grained microstructures have high ASTM grain size numbers (i.e., 6–10), while coarse-grain microstructures are identified by small ASTM grain size numbers (i.e., 1–3). In general, poor weld interface toughness corresponds with coarse grains (i.e., 1 or 2). Grain size analysis of the GMA welds of 12-mm-thick 12Cr stainless steel revealed there was considerable grain coarsening, in particular at the HTHAZ, with ASTM grain size numbers between 1 and 3, resulting in lower toughness data compared to those at the LTHAZ. The grain coarsening of the HAZ originating from the B6 joint was determined to be lower than the other welds (B9 and B8) — Fig. 3A. Less grain coarsening at B6 HAZ provided better toughness results at low temperatures compared to B9 and B8. Studies show that ferrite grain size has a marked effect on the impact properties of the HAZ, and ductile-to-brittle transition temperatures (DBTT) of 12% Cr steel increase with ferrite grain size (Refs. 12, 35, 51). In accordance with the literature, fine-grained structures enhance toughness properties. Grain coarsening can be restricted to microstructures with ASTM grain size numbers of 6 or higher with more proper control of the heat input.

Ferrite Content Results

When the chemical composition data of the base metal obtained by GDOES (Table 1) is taken into account, approximately 12.8 and 1.00 are calculated as Cr_{eq} and Ni_{eq}. According to the Balmforth and Lippold diagram (Ref. 3), the steel used here seems to consist of 80% ferrite and 20% martensite. Cr_{eq} of approximately 24.0, 20.5, and 23.9, and Ni_{eq} of 14.7, 11.8, and 13.9 for B9, B8, and B6, respectively, are calculated from the Balmforth and Lippold diagram, using all-weld-metal chemical composition data from Table 3, and the representative points are situated in austenite + martensite + ferrite region. Martensite islands as dark areas within the ferrite grains and some grain coarsening at the HAZs of the welds can be noticed —

Table 5 — Cylindrical All-Weld-Metal Tensile Properties of the Welds

Welding Process	Type of Consumable	Specimen Code	R_p (MPa)	R_m (MPa)	Elongation (%)	Reduction of Area (%)
GMAW	ER309LSi	B9TW1	329	565	44.5	51
		B9TW2	360	575	38.8	64
	ER308LSi	B8TW1	336	595	47.0	62
		B8TW2	316	589	47.2	65
	ER316LSi	B6TW1	483	573	?	53
		B6TW2	337	566	25.8	44

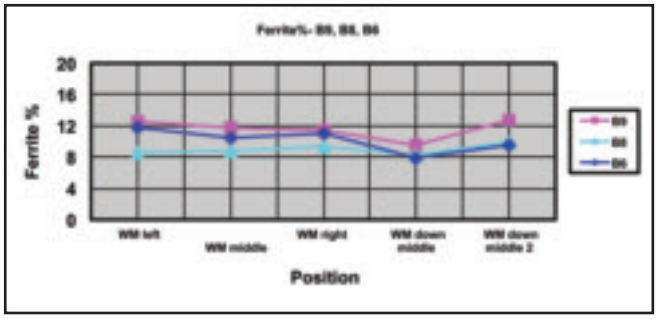

Fig. 6 — Ferrite content measurements of B9, B8, and B6 welds obtained by Feritscope®.

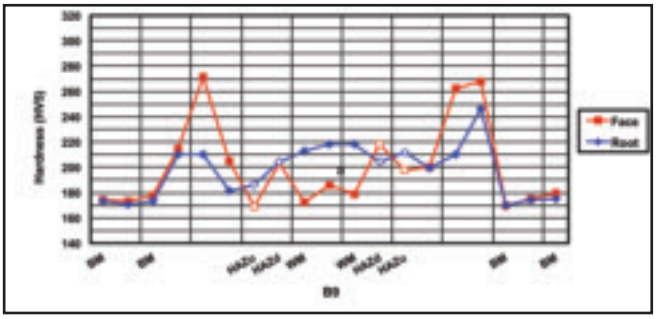

Fig. 7 — Hardness measurements on the cross sections of B9 joint.

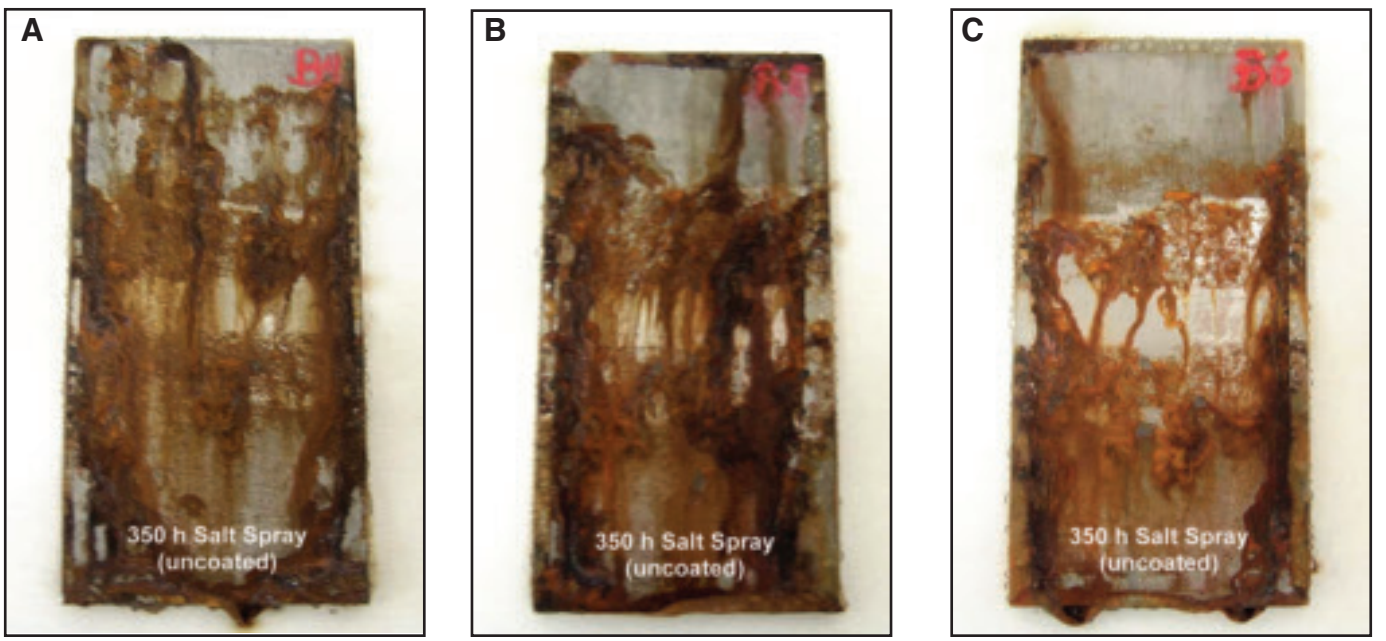

Fig. 8 — Uncoated salt spray test samples after 350 h. A — B9; B — B8; C — B6.

Figs. 1C, 2B, 3B. Again using data from Table 3 and the Schaeffler diagram (Ref. 1), Cr_{eq} of approximately 24.82, 21.24, and 22.20, and Ni_{eq} of 14.4, 11.1, and 13.48 for B9, B8, and B6, respectively, were calculated. With this diagram, between 5 and 10% ferrite is expected for the weld metals of B9, B8, and B6 joints, respectively. Depending on the ferrite content investigation by Feritscope®, weld metal ferrite content was measured at approximately between 9.5 and 12.7% for B9, while the results changed between 8.2 and 9.9% for B8, and between 7.9 and 11.8% for B6 (Fig. 7) due to the 309, 308, and 316 austenitic-type stainless steel filler metals used. The measured ferrite-% data are in general compatible, but a little higher than those predicted using the diagram.

Hardness Test Results

Relavant hardness measurements under 5-kg load over the weld cross sections of 12-mm-thick GMA welds made with ER309LSi, ER308LSi, and ER316LSi welding wires were taken. A representative hardness distribution is given for Weld B9 in Fig. 7. For each sample, HAZ measurements included two indentations 0.7 mm above and below the line of indentations for the left HAZ and for locations 0.7 mm below and above the line of indentations for the right HAZ. Weld metal hardness of the welds varied between 170 and 235 HV5. Maximum hardness values 275, 290, and 278 HV5 were measured at the HAZs of B9, B8, and B6 joints, respectively.

Transverse Tensile Test

Transverse tensile test results are given in Table 4. Test specimens prepared from each joint showed an overmatch with R_m values between 484 and 504 MPa. Fracture of the welds occurred at the base metal. Splitting of the base metal was observed close to the fracture surfaces parallel with the plate surface in accordance with the literature and is attributed to intergranular decohesion along ferrite-martensite grain boundaries (Refs. 13, 23).

All-Weld-Metal Tensile Test Results of Cylindrical Test Samples

Cylindrical test samples completely positioned at the weld metal and extracted from the respective welds in longitudinal direction were tested. The room-temperature tensile test results for the 12-mm-thick GMA welds made in modified 12% Cr stainless steel are given in Table 5.

Bend Test Results

None of the face and root bend samples failed during 180-deg bending. Harmless undercuts were observed.

Corrosion Properties

Uncoated and coated salt spray samples, respectively, after an exposure of 350 h and 1000 h are illustrated in Figs. 8 and 9. As a rule of thumb, damage caused in a salt spray test after 1000 h of exposure time may be extrapolated to about five years of atmospheric attack.

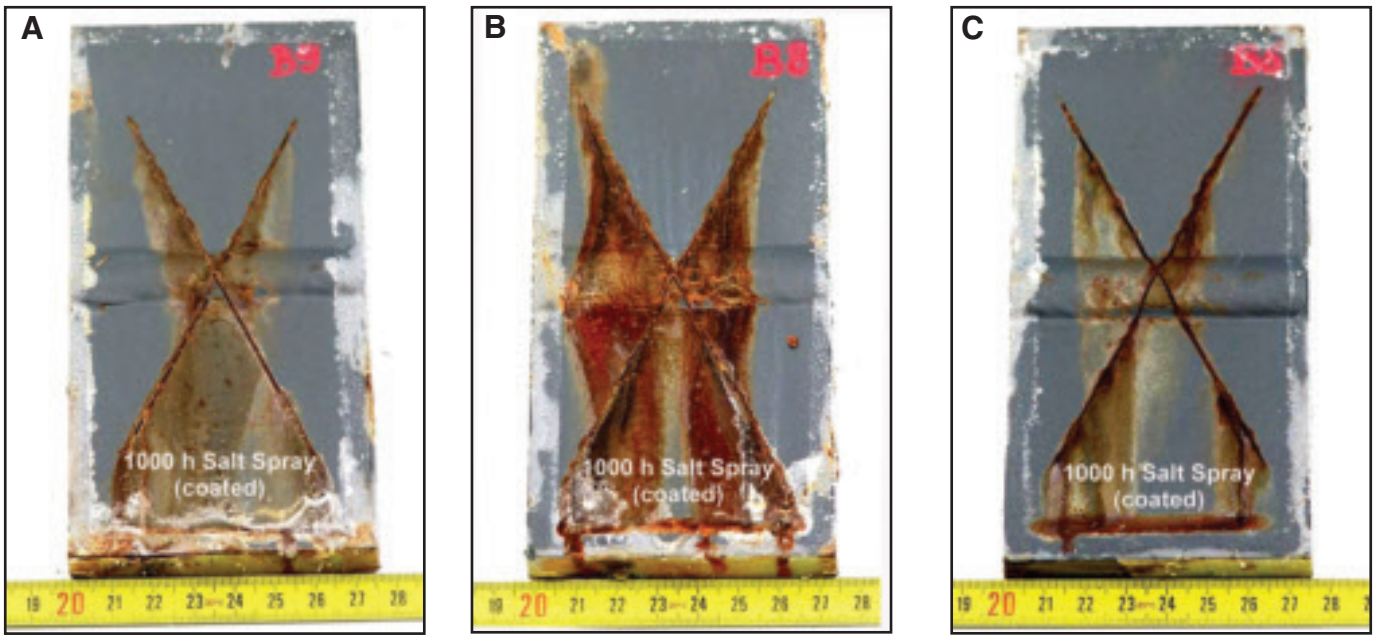

Fig. 9 — Coated salt spray corrosion test samples after 1000 h. A — B9; B — B8; C — B6.

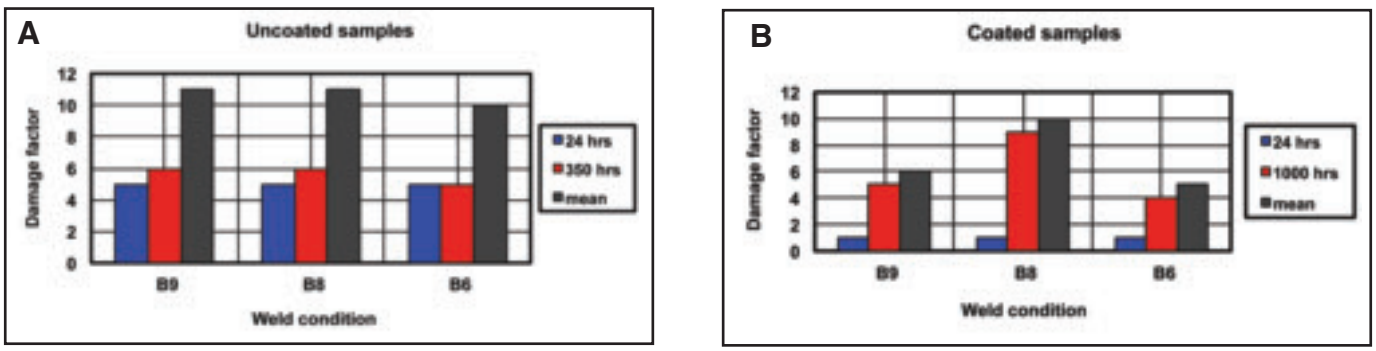

Fig. 10 — Damage factor during salt spray corrosion test. A — After 24 and 350 h for uncoated samples; B — after 24 and 1000 h for coated samples.

After an exposure of 24 h, uncoated salt spray test samples revealed red and brown attacks with drains from the weld metal. Drains increased when the exposure time increased. After an exposure time of 167 h, an increase of drains from welds was observed, with black-brown drains seen. A maximum increase was observed after 350 h. The test was ended for the related duration, since increasing the exposure time did not lead to an increase in corrosion. In the uncoated condition and after 350 h of exposure, Weld B6 revealed less deterioration than Welds B9 and B8. Weld B8 had the highest attack at the weld metal due to the least alloying element context compared to B9 and B6 weld metals. Thus, it was concluded that Weld B6 showed improved resistance with regard to B8 and B9.

Photographs after 1000 h of salt spray corrosion testing of coated samples are illustrated in Fig. 9. Short-term behavior (24 h) of coated samples heavily scratched across the welds, revealed small spots of corrosion at the scratched part of the welds. Damage systematically worsened in the course of testing till about 140 h of exposure. Long-term behavior of coated samples revealed some corrosion at the scratch in case of all welds. The applied coating provided a good protection, as in general only scratched regions deteriorated. The influence of the type of consumable is very detectable and confirmed on the samples after the test, as Weld B6 proved to be the most resistant and Weld B8 the least resistant — Fig. 8A–C and Fig. 9A and B. After 1000 h, the GMA welds on modified 12% Cr stainless steel were found resistant enough for mild environments.

Some ranking between welds has been given, but this should be treated with great care as interpretation of such type of observations is often distorted by personal bias. The purpose, therefore, is not to distinguish between good and bad combinations but rather between resistant and less-resistant welds. Each data describes the changes in observations, i.e., any worsening or new observations, with regard to the former period. Taking this into account, Fig. 10A summarizes the damage factor due to the weld combinations after 24 and 350 h of salt spray testing of uncoated samples. Figure 10B represents the mean damage factor of short and long time exposure after 24 and 1000 h of salt spray testing of coated samples. Most damage was observed at Weld B8 as observed in Fig. 10.

Coated samples after 3120 h of blister testing are illustrated in Fig. 11. At each observation for the blister sample, air temperatures were noted, ranging from minimum about 0° to maximum 42°C, as this parameter can have a great effect on corrosion response. Only Weld B8 showed some small spots at the scratch already after 360 h, then the sample succeeded practically in preventing further damage to occur. Weld B6 was totally resistant against atmospheric attack over a period of 2500 h even when damaged by a severe scratch across the entire welded joint.

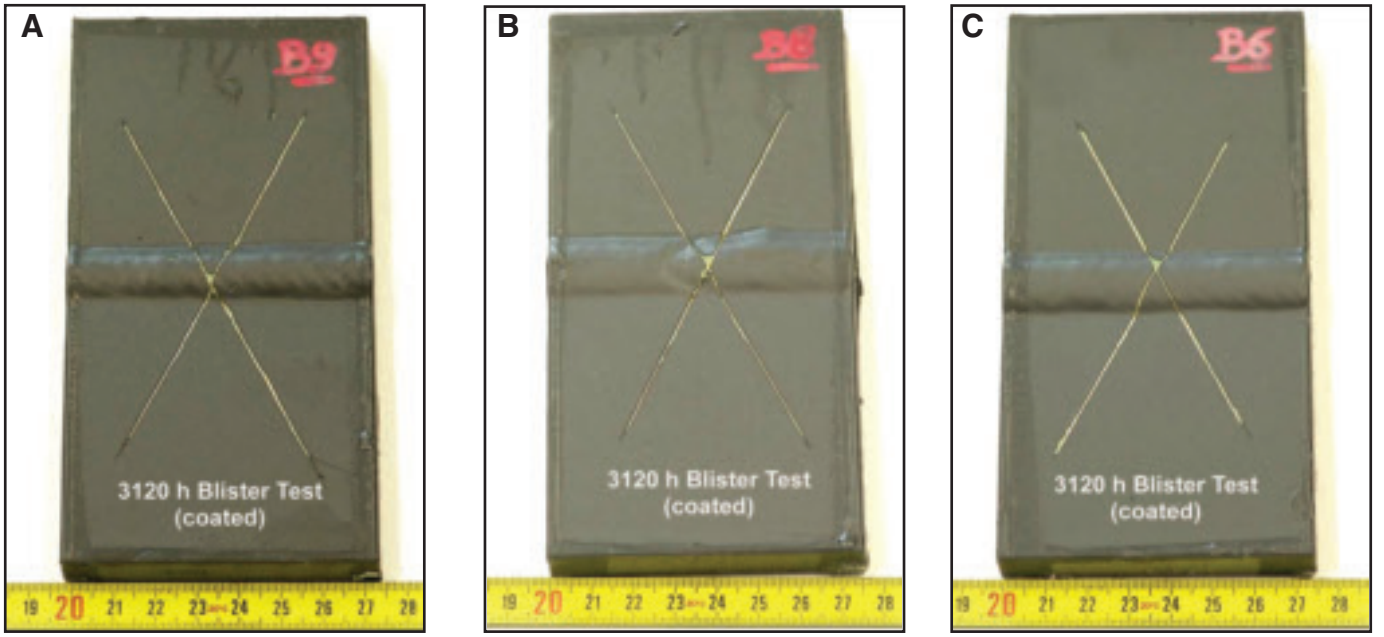

Fig. 11 — Coated blister corrosion test samples after 3120 h. A — B9; B — B8; C — B6.

From the blister test samples, it is concluded that Weld B6 made with 316LSi consumable was again the most resistant against atmospheric attack over periods that cover both winter and summer seasons. In general, corrosion behavior is affected by the type of consumables certainly in protected condition and artificially damaged across the entire weld. In these cases, 316LSi filler metal improves the corrosion resistance of the whole system with regard to 309 or 308 filler metals that, due to its lower alloying, demonstrate an inferior corrosion behavior.

Conclusions

The following conclusions of this research work concerning the GMAW of 12-mm-thick modified 12% Cr stainless steel conforming to EN 1.4003 and UNS S41003 were drawn:

Modified X2CrNi12 ferritic stainless steel complying with EN10088 can be fabricated with a low level of carbon and impurities. In general, defect-free joining of 12-mm-thick X2CrNi12 stainless steel is feasible by GMAW. The weld metal in the present welds without exception was overmatched in tensile strength. The 180-deg bending of the face and root bend samples revealed no defects except harmless small undercuts.

Welds B6 and B9 produced with 316LSi and 309LSi austenitic welding wires, respectively, have proven that adequate low-temperature impact toughness is achievable down to –20°C, which is very encouraging. Only Weld B8 produced with 308LSi consumable failed at low temperatures because of insufficient mean toughness at the weld interface notch position. However, HTHAZ toughness at subzero temperatures has been improved by PWHT for 30 min at 720° and 750°C, which is promising.

The major challenge of the stainless steel is the tendency for grain coarsening at the HTHAZ. Grain coarsening had no negative effect on tensile and bend properties, but the HTHAZ impact toughness may be disappointing, which depends on the amount of grain-coarsened microstructures. Microscopic investigations have shown that if the grain coarsening could be restricted to microstructures with ASTM grain size numbers of 6 or higher with a more controlled heat input range, welds would be much tougher. The correlation between microstructure and impact toughness was defined as less substantial grain coarsening and was determined for Weld B6, which exhibited higher toughness values. Considerable grain coarsening was found for B8, which failed in toughness at low temperature. Hardness at the HAZs of this steel can easily be limited to 300 HV5.

Atmospheric corrosion resistance of the welds is also very promising even when evaluated under severe circumstances, such as artificial damage. Under pure atmospheric conditions, all welds demonstrated the possibility to prevent further development of corrosion once initiated. Weld B8 was classified as less corrosion resistant than the welds B9 and B6 with 309 and 316 consumables. In particular, 316 filler metal provides the best corrosion resistance.

Interpreting all data gathered within this work, the effects of the consumable are mostly observed for the toughness and corrosion properties. Taking this into account, it can be recommended to use 309 and 316 austenitic consumables for gas metal arc welding of 12-mm-thick modified 12Cr stainless steel conforming to EN 1.4003 grade in the areas where impact or shock is anticipated and adequate atmospheric corrosion is required.

Acknowledgments

The authors would like to acknowledge the help of all colleagues at the Belgian Welding Institute. In addition, the support of IWT, ArcelorMittal Belgium, University of Ghent, WTCM, and Bombardier Eurorail are very much appreciated and acknowledged for their contribution and technical support.

References

1. Lippold, J. C., and Kotecki, D. J. 2005. *Welding Metallurgy and Weldability of Stainless Steels*, 1st ed., John Wiley & Sons, New Jersey.

2. Shanmugam, K., Lakshminarayanan, A. K., and Balasubramanian, V. 2009. *International Journal of Pressure Vessels and Piping* 86: 517–52.

3. Balmforth, M. C., and Lippold, J. C. 2000. *Welding Journal* 79(12): 339-s.

4. J. R. Davis, ed. 1994. *ASM Specialty Handbook — Stainless Steels*, ASM International, Materials Park, Ohio.

5. Folkhard, E. 1984. *Welding Metallurgy of Stainless Steels*, Springer-Verlag, Wien, New York.

6. Nirosta, N. N. 4003—The winning formula of modern steel applications. Product cat-

alog, Tyssen Krupp Nirosta, Germany.
7. Kaluc, E., Taban, E., Paslanmaz, C., and Gelistirilen, Yeni Turleri ve Kaynak, Edilebilirlikleri. 2007. MMO 2007/461, ISBN: 978-9944-89-438-8.
8. Akita, M., Nakajima, M., Tokaji, K., and Shimizu, T. 2006. *Materials and Design* 27: 92–99.
9. Meadows, C., and Fritz, J. D. 2005. *Welding Journal* 84: 25–30.
10. Gordon, W., and Van Bennekom, A. 1996. *Materials Science and Technology* 12: 126–131.
11. Woollin, P. 1994. *Welding and Metal Fabrication* 62: 18–26.
12. Gooch, T. G., and Ginn, B. J. 1988. *The Welding Institute Members Report* 373/ 1988 (7): 30.
13. Thomas, C. R. 1983. Structure and properties of a duplex ferritic-martensitic stainless steel. Lula, R. A., ed., *Duplex Stainless Steels, Conference Proc*., ASM, 649–664.
14. Cavazos, J. L. 2006. *Mater Charact*. 56: 96.
15. Marshall, A. W., and Farrar, J. C. M. IIW Doc: IX-1975-00, IXH-494-2000.
16. Dhooge, A., and Deleu, E. 2005. 12% Cr roestvast staal voor primaire constructies. BIL/NIL Lassyposium, Het Pand, Ghent, Belgium, Session 7.
17. Dhooge, A., and Deleu, E. 2005. Ferritic stainless steel X2CrNi12 with improved weldability for structural applications. *Stainless Steel World 2005 Conference & Expo*, Netherlands, p. 160.
18. Greef, M. L., and du Toit, M. 2006. *Welding Journal* 85: 243-s to 251-s.
19. du Toit, M., van Rooyen, G. T., and Smith, D. An overview of the heat affected zone sensitization and stress corrosion cracking behaviour of 12% chromium type 1.4003 ferritic stainless steel. IIW Doc IX-2213-06, IIW Doc. IX-H-640-06.
20. Karjalainen, P., Kyrölainen, A., Kauppi, T., and Orava, U. 1992. Mechanical properties and weldability of new 12Cr type stainless steel sheets. *Applications of Stainless Steels,* pp. 225–234, Stockholm, Sweden.
21. Castner, H. R. 1977. *Welding Journal* 56: 193-s to 199-s.
22. Irvine, K. J., Crowe, D.J., and Cantab, M. A. 1960. AIM, Pickering FB. *Journal of the Iron and Steel Institute,* pp. 386–405.
23. Taban, E. 2007. Weldability and properties of modified 12Cr ferritic stainless steel for structural applications. PhD thesis, Kocaeli University.
24. NN. 2004. CLC 4003. Product Catalogue; Arcelor Group, France.
25. NN. 2002. Columbus stainless technical data 3Cr12. Columbus Stainless Pty. Ltd.
26. Kotecki, D. J. 2005. Stainless Q&A, *Welding Journal* 84: 14.
27. Topic, M., Allen, C., and Tait, R. 2007. *Int. J. of Fatigue* 29: 49–56.
28. van Warmelo, M., Nolan, D., and Norrish, J. 2007. *Materials Science and Engineering* A 464, pp. 157–169.
29. Ball, A., Chauhan, Y., and Schaffer G. B. 1987. *Materials Science and Technology* 3: 189–196.
30. Thomas, C. R., and Hoffmann, J. P. 1982. Metallurgy of a 12% chromium steel. N. R. Comins and J. B. Clark, eds. *Speciality Steels and Hard Materials Conference,* Pretoria, South Africa, pp. 299–306.
31. Kaltenhauser, R. H. 1971. *Met. Eng. Quarterly* 11: 41–47.
32. Aghion, E., and Ferreira, J. 1993. *Canadian Metal Quar*. 32: 369.
33. Ball, A, Chauhan, Y., and Schaffer G. B. 1987. *Mater Sci and Tech*. 3: 189.
34. Bennett, P. 1991. *Materials Australia* (6): 15.
35. Meyer, A. M., and du Toit, M. 2001. *Welding Journal* 80: 275-s.
36. Moore, P. 1997. *Australasian Weld J.* 42: 22.
37. IAF Editor. 2000. *Welding and Metal Fabrication*, p. 18.
38. Marini, A., and Knight D. S. 1994. *Corr and Coat SA*. (3): 4.
39. Maxwell, D. K. 1997. *Mater Australia* (11/12): 20.
40. van Lelyveld, C., and van Bennekom, A. 1995. *Stainless Steel* (9/10): 16.
41. Taban, E., Deleu, E., Dhooge, A., and Kaluc, E. 2007. *Kovove Materialy-Metallic Materials* 45: 67–73.
42. Taban, E., Deleu, E., Dhooge, A., and Kaluc, E. 2008. *Science and Technology of Welding and Joining* 13(4): 327–334.
43. Taban, E., Deleu, E., Dhooge, A., and Kaluc, E. 2006. Mechanical and microstructural properties of welded X2CrNi12 ferritic stainless steel. DVS GST. *Schweissen und Schneiden.* Germany, (9): 74–79.
44. Deleu, E., Dhooge, A., Taban, E., and Kaluc, E. 2009. *Welding in the World* 53(9-10): R198-R208.
45. Taban, E., Deleu, E., Dhooge, A., and Kaluc, E. 2008. *Welding Journal* 87(12): 291-s to 297-s.
46. Taban, E., Deleu, E., Dhooge, A., and Kaluc, E. 2009. *Materials and Design* 30(10): 4236–4242.
47. Taban, E., Dhooge, A., and Kaluc, E. 2009. *Materials and Manufacturing Processes* 24 (6): 649–656.
48. Taban, E., Deleu, E., Dhooge, A., and Kaluc, E. 2009. *Materials and Design*, 30(4): 1193–1200.
49. Taban, E., Deleu, E., Dhooge, A., and Kaluc, E. 2008. *Welding and Cutting* 7: 354–359.
50. Lakshminarayanan, A. K., and Balasubramanian, V. 2010. *Steel Research International* 81(11): 1023–1033.
51. Krauss, G. 1989. *Steels: Heat Treatment and Processing Principles*. ASM International, Materials Park, Ohio.

Opportunities to Contribute to AWS Welding Standards and Codes

NOTE: LEARN MORE ABOUT TECHNICAL COMMITTEES AND APPLY FOR MEMBERSHIP ONLINE AT *WWW.AWS.ORG/TECHNICAL/JOINTECHCOMM.HTML*.

Robotic and Automatic Welding

The **D16 Committee on Robotic and Automatic Welding** seeks general interest and educators to help revise its documents. Contact B. McGrath, *bmcgrath@ aws.org;* ext. 311.

Soldering; Joining Nickel Alloys

The **G2C Subcommittee on Nickel Alloys** to review B2.3/B2.3M, *Specification for Soldering Procedures and Performance Qualification.* Contact S. Hedrick, *steveh@ aws.org*; ext. 305.

Local Heat Treating of Pipe Work

The **D10P Subcommittee for Local Heat Treating of Pipe** seeks members. Contact B. McGrath, *bmcgrath@aws.org;* ext. 311.

Magnesium Alloy Filler Metals

A5L Subcommittee on Magnesium Alloy Filler Metals to assist in the updating its document. Contact R. Gupta, *gupta@aws.org,* ext. 301.

Thermal Spray

C2 Committee on Thermal Spraying seeks educators, general interest, and users to update its documents. Contact E. Abrams, *eabrams@aws.org*; ext. 307.

Oxyfuel Gas Welding and Cutting

C4 Committee on Oxyfuel Gas Welding and Cutting seeks general interest and educators to help review its documents. Contact E. Abrams, *eabrams@aws.org*; ext. 307.

Surfacing Industrial Mill Rolls

D14H Subcommittee on Surfacing and Reconditioning of Industrial Mill Rolls to revise AWS D14.7, *Recommended Practices for Surfacing and Reconditioning of Industrial Mill Rolls.* Contact M. Rubin, *mrubin@aws.org*, ext. 215.

Automotive Welding

The **D8 Committee on Automotive Welding** seeks members to help prepare standards on all aspects of welding in the automotive industry. Contact E. Abrams, *eabrams@aws.org*; ext. 307.

Resistance Welding Equipment

The J1 Committee on Resistance Welding Equipment seeks educators, general interest, and users to help develop its documents on controls, installation and maintenance, calibration and resistance welding fact sheets. Contact E. Abrams, *eabrams@aws.org*; ext. 307.

Welding Handbook

Volunteers with experience in welding copper, lead, zinc, and titanium are sought to help update the *Welding Handbook*. Contact A. O'Brien, *aobrien@ aws.org*; ext. 303.